

Threshold vortex formation and trapping fields in small high- T_c superconducting particles

E. V. Blinov, L. S. Vlašenko, Yu. A. Kufaev, E. B. Sonin, Yu. P. Stepanov, A. K. Tagantsev, and V. G. Fleisher

A. F. Ioffe Physicotechnical Institute, Russian Academy of Sciences

(Submitted 13 August 1992)

Zh. Eksp. Teor. Fiz. **103**, 617–628 (February 1993)

The Gibbs thermodynamic potential is used to investigate theoretically the possibility of vortex formation in superconducting particles which have different shapes and whose transverse size is smaller than the penetration depth. Expressions are derived for the threshold fields for vortex formation and trapping during cooling with and without an external field. They show that the threshold fields depend on the radius of the particles. This agrees with an experiment performed on powdered high- T_c superconductors with different particle-size distributions.

1. INTRODUCTION

It was shown in Ref. 1 that the trapping of magnetic flux in powdered high- T_c superconductors with particles of order several microns depends on the particle size in the sample. The trapping probability is extremely low in fields $H < \Phi_0/S_k$, where Φ_0 is the magnetic-flux quantum and S_k is the cross sectional area of the particle.

In addition, in Ref. 2 Afanas'ev *et al.* observed, while investigating the hf properties of such powdered superconductors in weak magnetic fields, that the Q of the hf oscillatory circuit into which the high- T_c superconducting sample was inserted depends on the constant magnetic field and near zero field the Q has a singularity, i.e., as the constant magnetic field H increases (with $H < 1$ Oe), Q at first increases and only then decreases, as observed for ceramic high- T_c superconductors.^{3–5} Trapping of single magnetic vortex filaments significantly affects the hf properties of powdered high- T_c superconductors near $H = 0$.

In the present paper we study the formation and trapping of magnetic flux by small particles with radius $R \ll \lambda$, where λ is the penetration depth, and we investigate the effect of the trapped magnetic field on the hf absorption by a finely dispersed high- T_c superconductor in weak magnetic fields.

2. THEORY

2.1. Basic assumptions

We note first that in superconductors whose transverse dimensions are less than the penetration depth λ quantization of magnetic flux does not occur. Indeed, the magnetic flux Φ is determined by the expression⁶

$$\Phi = \int \mathbf{h} d\mathbf{S} = \Phi_0 n - \frac{4\pi\lambda^2}{c} \oint \mathbf{j} d\mathbf{l}, \quad (1)$$

where $n = 0, 1, 2, \dots$. When magnetic flux penetrates into a superconductor with small transverse size the circulation of the current along the surface of the superconductor is non-zero ($\oint \mathbf{j} d\mathbf{l} \neq 0$), and for this reason the trapped magnetic flux is not a multiple of the magnetic-flux quantum Φ_0 . This is very important for flux penetration into thin films⁷ as well as for high- T_c superconducting powders with particle sizes $R < \lambda$.

In the case of samples of small transverse size the cur-

rent can be expressed in terms of the gradient $\nabla\varphi$ of the phase as

$$\mathbf{j} = \frac{c}{4\pi\lambda^2} \left(\frac{\Phi_0}{2\pi} \nabla\varphi \right), \quad (2)$$

and it can be assumed that the free energy F is determined mainly by the kinetic energy of these currents

$$F = \frac{1}{4\lambda^2} \left(\frac{\Phi_0}{2\pi} \right)^2 \int (\nabla\varphi)^2 d^3r. \quad (3)$$

The Gibbs thermodynamic potential G can be related to the angular momentum of the currents in the sample as

$$G = F - \frac{1}{4\pi} \int \mathbf{h}(r)\mathbf{H} d^3r = F - \frac{2\pi}{c} \int \mathbf{H}[\mathbf{r}\mathbf{j}] d^3r, \quad (4)$$

where \mathbf{H} is the external magnetic field and \mathbf{h} is the field generated in the sample by the current \mathbf{j} . A distinctive feature of this problem is that the current in this equation is determined only by the shapes of the sample and the vortex filament and it does not depend on the external magnetic field. This enables Eq. (4) to be used effectively in the further analysis.

2.2. Magnetic vortex in a cylinder

For a straight vortex at a distance r from the center of a thin cylinder with radius $R \ll \lambda$, the Gibbs potential per unit length is

$$G(r) = \frac{\Phi_0^2}{(4\pi\lambda)^2} \ln \frac{R^2 - r^2}{\xi R} - \frac{\Phi_0}{(4\pi\lambda)^2} \pi(R^2 - r^2)H. \quad (5)$$

Here ξ is the transverse size of the flux and H is the intensity of the magnetic field.

Up to values $H = \Phi_0/\pi R^2$ this function is monotonic and does not have a minimum (Fig. 1, curve 1). In other words, the vortex cannot be stable inside the cylinder.

As the magnetic field increases, a minimum of the thermodynamic potential appears in fields above

$$H^* = \Phi_0/\pi R^2 \quad (6)$$

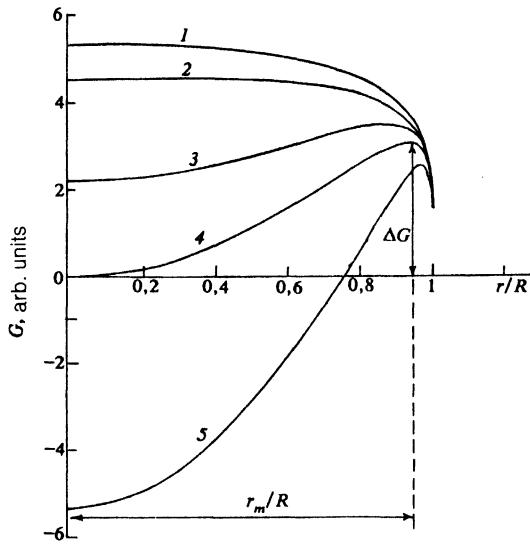


FIG. 1. Thermodynamic potential G in a particle of radius R for different values of the magnetic field H : $H = 0$ (1), $H = H^*$ (2), $H^* < H < H^{**}$ (3), $H = H^{**}$ (4), and $H > H^{**}$ (5).

(Fig. 1, curve 2) at the center of the cylinder ($r = 0$) and a magnetic vortex filament can form.

We now find the magnetic field H^{**} for which the energy at the center of the cylinder is equal to the energy on the outer surface of the cylinder (curve 4 in Fig. 1). We note that this same condition corresponds to the classical definition of the lower critical field H_{c1} for a bulk superconductor.⁶ It follows from Eq. (5) that

$$H^{**} = \frac{\Phi_0}{\pi R^2} \ln \frac{R}{\xi}. \quad (7)$$

In this case a barrier ΔG given by

$$\Delta G = \frac{\Phi_0^2}{(4\pi\lambda)^2} \ln \frac{R}{\xi} \quad (8)$$

must be overcome in order for the vortex filament to penetrate into the cylinder (Fig. 1).

This is the Bean-Livingston barrier for a thin cylinder. The role of such a barrier in vortex penetration into bulk samples was investigated in Refs. 8–10. We show in our work that this barrier also plays a significant role in magnetic-flux penetration into small superconducting particles. In order to analyze this phenomenon further we must switch from a cylinder to a sphere with a small radius.

2.3. Rectilinear magnetic vortex line in a small sphere

Analysis of the problem of magnetic flux in a small superconducting sphere gives qualitatively similar results. Here, however, a number of features which change the values of H^* and H^{**} must be taken into account.

A distinguishing feature of a vortex in a sphere is that the free energy appearing in the thermodynamic potential is affected primarily by the change in the length of the flux line as the flux moves away from the center of the sphere.

In the case of a straight vortex (Fig. 2a) the thermody-

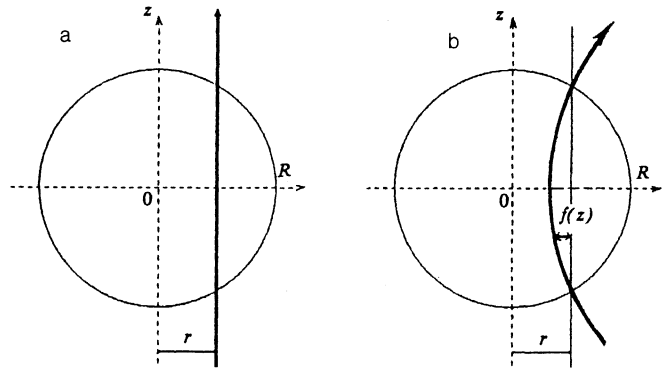


FIG. 2. Vortex filament in a sphere: rectilinear flux line (a) and curved flux line (b).

amic potential [Eq. (4)], calculated taking into account the length of the vortex filament, has the form

$$G(r) = 2 \left(\frac{\Phi_0}{4\pi\lambda} \right)^2 \left[(R^2 - r^2)^{1/2} - \frac{2}{3a^2} (R^2 - r^2)^{3/2} \right] \ln \frac{R_v}{\xi}, \quad (9)$$

where R is the radius of the sphere ($R \ll \lambda$), $a^2 = (\Phi_0/\pi H) \ln(R_v/\xi)$, and the cutoff radius R_v for vortex filaments which are not located too close to the edge of the sample is chosen to be of the order of the radius of the sphere R .

For $H > (\Phi_0/2\pi R^2) \ln(R/\xi)$ a minimum of the thermodynamic potential develops at the center of the sphere (Fig. 1, curve 3), and starting with this field

$$H^* = \frac{\Phi_0}{2\pi R^2} \ln \frac{R}{\xi} \quad (10)$$

the vortex can be trapped as the sphere is cooled in a magnetic field.

The magnetic field at which the energy of the vortex at the center of the sphere is equal to the energy at the outer surface of the sphere (Fig. 1, curve 4) is

$$H^{**} = \frac{3}{2} \frac{\Phi_0}{\pi R^2} \ln \frac{R}{\xi}, \quad (11)$$

and the height of the potential barrier at distance $r_m = (R^2 - a^2/2)^{1/2}$ from the center of the sphere is given by the expression

$$\Delta G = \frac{4}{3\sqrt{3}} \left(\frac{\Phi_0}{4\pi\lambda} \right)^2 R \ln \frac{R}{\xi}. \quad (12)$$

2.4. Curved vortex filament in a sphere with a small radius

Another distinguishing feature of a vortex filament in a sphere is that the flux line can bend as it moves away from the center of the sphere. The configuration of a vortex filament in a sphere can be described by the function $f(z)$ (Fig. 2b) which is determined by minimizing the thermodynamic potential

$$G(r) = \left(\frac{\Phi_0}{4\pi\lambda} \right)^2 \ln \frac{R_v}{\xi} \int_{-\mathcal{R}}^{\mathcal{R}} \left\{ \sqrt{1 + f'(z)^2} - \frac{R^2 - z^2 - [r - f(z)]^2}{a^2} \right\} dz, \quad (13)$$

$$\mathcal{R} = \sqrt{R^2 - r^2}$$

and from the boundary condition that the flux be perpendicular to the surface of the sphere.

The shape of the vortex filament is determined by varying this expression with respect to the function $f(z)$. This gives the differential equation

$$-\frac{d}{dz} \left[\frac{f'(z)}{\sqrt{1 + (f'(z))^2}} \right] - \frac{2[r - f(z)]}{a^2} = 0. \quad (14)$$

In the case of vortex filament located close to the axis of the sphere ($r \ll R$) this nonlinear equation becomes a linear equation whose solution is

$$f(z) = r - \frac{ra}{\sqrt{2(R^2 - r^2)}} \frac{\text{ch}(z\sqrt{2}/a)}{\text{sh}[\sqrt{2}(R^2 - r^2)/a]}. \quad (15)$$

It should be noted that this problem can be solved only for extremal positions of the vortex filament. For this reason the condition

$$1 = \frac{R\sqrt{2}}{a} \text{th} \frac{R\sqrt{2}}{a}, \quad (16)$$

under which the solution of the problem of minimizing the potential (13) can satisfy simultaneously the two boundary conditions $f(z) = 0$ and $f'(z) = -r/R$ with $z = \pm \sqrt{(R^2 - r^2)} \approx \pm R$ corresponds to the field

$$H^* = 0,72 \frac{\Phi_0}{\pi R^2} \ln \frac{R}{\xi}, \quad (17)$$

in which the vortex filament assumes an extremal position near the axis of the sphere corresponding to maximum energy, i.e., this field is a refined value of the field H^* calculated previously for a straight vortex.

It is also possible to determine the extremal position corresponding to maximum energy in the other limiting case $r \approx R$, i.e., when the vortex is located at the edge of the sphere

$$f(z) = \frac{a^2}{2R} \left[1 - \left(\frac{2R}{a^2} z \right)^2 \right]^{1/2}. \quad (18)$$

This solution corresponds to a vortex filament in the form of a semicircle supported by the surface of the sphere, and the potential barrier as a function of the external magnetic field has the form

$$\Delta G(H) = 0,25 \left(\frac{\Phi_0}{4\pi\lambda} \right)^2 \frac{\Phi_0}{RH} \ln^2 \frac{R_v}{\xi}. \quad (19)$$

In this formula the radius of the semicircle must be taken as the cutoff parameter R_v in the argument of the logarithm: $R_v \approx a^2/2R$.

As the magnetic field increases further, the barrier gradually decreases in height and vanishes completely in fields $H \sim \Phi_0/R\xi$.

2.5. Threshold fields for vortex filament formation and trapping in a sphere

The case of a curved vortex filament in a small superconducting sphere studied in the preceding section takes into account the characteristics of magnetic flux in small high- T_c superconducting particles, in leading order, and for this reason the formulas derived there can be used to find the threshold magnetic fields in which magnetic flux is trapped in an isolated particle.

The expression for the external magnetic field H_{th}^{ZFC} in which flux can penetrate into a sphere initially in the Meissner state can be obtained from Eq. (19) under the condition $\Delta G(H) = kT$, where k is Boltzmann's constant and T is the temperature, and taking into account $\ln(R_v/\xi) = \ln(a^2/2R\xi) \approx \ln(R/\xi) + \ln(kT\lambda^2/\Phi_0^2 R) \approx \ln(R/\xi)$. Then

$$H_{th}^{ZFC} = 0,25 \left(\frac{\Phi_0}{4\pi\lambda} \right)^2 \frac{\Phi_0}{RkT} \ln^2 \frac{R}{\xi}. \quad (20)$$

When the cooling occurs in a magnetic field (FC), however, the minimum field H_{th}^{FC} in which flux can be trapped in a sphere, is, in accordance with Eq. (15),

$$H_{th}^{FC} = 0,72 \frac{\Phi_0}{\pi R^2} \ln \frac{R}{\xi}. \quad (21)$$

We note that when the sample is cooled in a magnetic field $H > H^*$ the appearance of a minimum in the thermodynamic potential creates conditions under which a vortex filament can form and be trapped in a particle. Internal pinning centers also provide the same possibility. In the latter case, however, the threshold trapping field should be independent of particle size and this disagrees with experiment.¹ Thus it can be concluded that the thermodynamic potential determines the threshold trapping field.

It is obvious that after the external field is switched off, flux is trapped by pinning centers. It is also obvious that the difference in the mechanism of flux penetration into a sample initially cooled in zero field (ZFC) is that a barrier must be overcome. This process occurs in a significantly stronger field, and when the field is switched off, flux is trapped by volume pinning centers.

3. EXPERIMENTAL PROCEDURE

The experiments were performed at $T = 77$ K with two samples, prepared from Y-Ba-Cu-O ceramic by pulverizing the ceramic and separating the powders according to particle size. The samples contained about 50 mg of the powder. The particle-size distribution in the samples is shown in Fig. 3. The average particle size in the first sample was $S_{av} \approx 16 \mu\text{m}^2$ ($R_{av} = 2.25 \mu\text{m}$); in the second sample $S_{av} \approx 25 \mu\text{m}^2$ ($R_{av} = 2.8 \mu\text{m}$). The maximum particle sizes in the samples were 32 and 55 μm^2 , respectively. The samples were placed in the coil of an oscillatory circuit tuned to the frequency 3.5 MHz. An alternating magnetic field $\mathbf{H}_1 \sin \omega t$ was produced by another coil, arranged coaxially with the coil of the oscillatory circuit. The constant magnetic field H was directed parallel to \mathbf{H}_1 and could take on values up to ± 100 Oe. The external magnetic field components transverse to \mathbf{H} were compensated to 0.02–0.03 Oe.

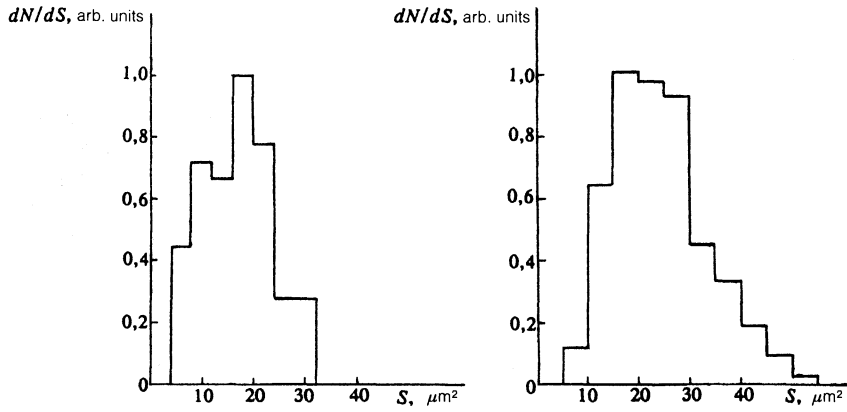


FIG. 3. Particle-size distribution in the samples.

The signals corresponding to changes ΔU produced in the amplitude of the hf voltage in the circuit with the sample when the field H was scanned near the zero value were observed by a method similar to that described in Ref. 2. The signals were recorded with the help of low-frequency modulation of the magnetic field and synchronous detection.

The remanent magnetization of the sample was measured with the help of a SQUID magnetometer.

4. EXPERIMENTAL RESULTS AND DISCUSSION

The signal amplitude ΔU versus the constant field H in which the sample was transferred into the superconducting state with FC is shown in Fig. 4a for a sample with average particle size $S_{av} \approx 16 \mu\text{m}^2$.

We note that the observed signal is a superposition of signals from separate particles, i.e., $\Delta U = \Sigma \Delta U_k$. A separate particle contributes to the observed signal as long as the particle is in the Meissner state and has not trapped any flux. For this reason, as the field H increases, the condition $H = \Phi_0/S_k$ is satisfied successively for all particles in the sample, starting with the largest ones, and the form of the magnetic field dependence $\Delta U(H)$ is determined by the particle-size distribution. It is easy to see that the field \bar{H}_{th} in which the decrease in the signal as a function of the field $d(\Delta U)/dH$ is maximum corresponds to trapping of magnetic flux by particles with area S_{av} . As one can see from Fig. 4a, the signal amplitude starts to decrease in fields $H \approx 1$ Oe, and $\bar{H}_{th}^{FC} \approx 3.5$ Oe.

Figure 4b shows the field dependence $\Delta U(H)$ obtained for the same sample in the case when the sample was initially cooled in zero magnetic field (ZFC) and then magnetized successively in the fields H . In this case trapping of magnetic flux and therefore a decrease in the signal amplitude ΔU should be observed in accordance with the formula (20).

In this case the field corresponding to trapping of the magnetic flux by the largest particles in the sample is about 10 Oe, and $\bar{H}_{th}^{ZFC} \approx 35$ Oe. Comparing Figs. 4a and 4b we find for this sample $\bar{H}_{th}^{ZFC}/\bar{H}_{th}^{FC} \approx 10$.

An expression for this ratio can be obtained from the formulas (20) and (21):

$$\frac{\bar{H}_{th}^{ZFC}}{\bar{H}_{th}^{FC}} = \frac{25}{72} \left(\frac{\Phi_0}{4\lambda} \right)^2 \frac{R}{\pi kT} \ln \frac{R}{\xi}. \quad (22)$$

As follows from Eqs. (20)–(22), as the average particle size in the sample increases, the quantities \bar{H}_{th}^{FC} and \bar{H}_{th}^{ZFC} should decrease and the ratio $\bar{H}_{th}^{ZFC}/\bar{H}_{th}^{FC}$ should increase.

Figure 5 shows the field dependence $\Delta U(H)$ for FC and ZFC. The curves were obtained for a sample with average particle size $S_{av} \approx 25 \mu\text{m}^2$ in the field (a) and without the field (b).

According to the figure, as the average particle size in-

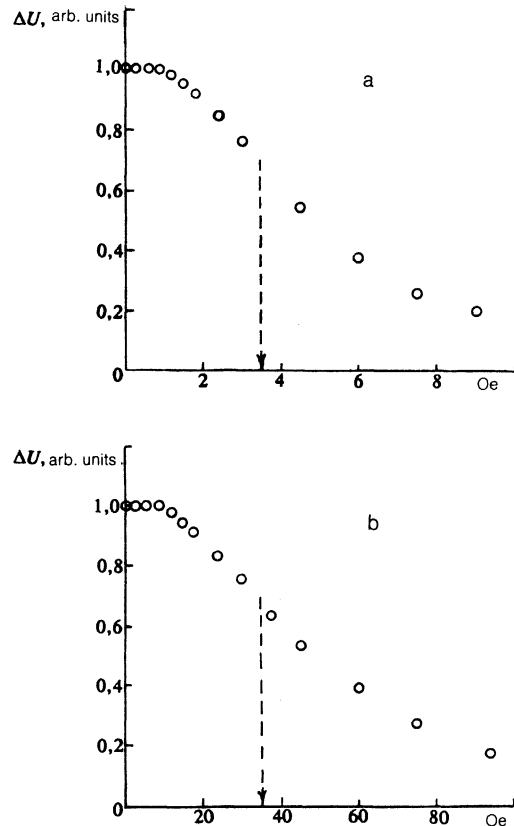


FIG. 4. HF absorption signal ΔU as a function of the intensity of the magnetic field with FC (a) and after ZFC (b) for a sample with average particle size of $16 \mu\text{m}^2$. The arrows mark the values of \bar{H}_{th}^{FC} and \bar{H}_{th}^{ZFC} , respectively.

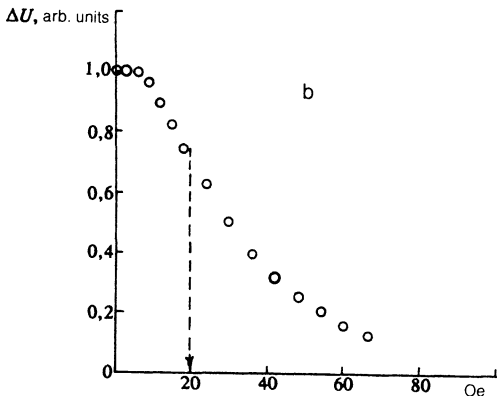
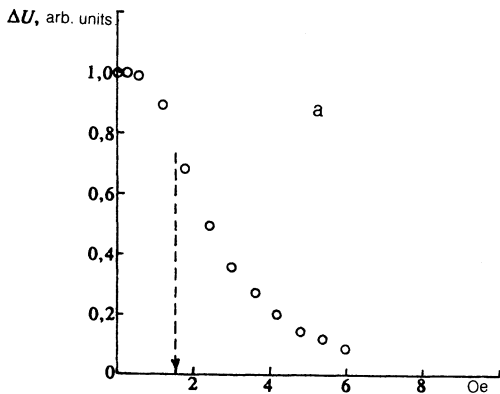


FIG. 5. HF absorption signal ΔU as a function of the intensity of the magnetic field with FC (a) and after ZFC (b) for a sample with average particle size of $25 \mu\text{m}^2$. The arrows mark the values of $\overline{H_{\text{th}}^{\text{FC}}}$ and $\overline{H_{\text{th}}^{\text{ZFC}}}$, respectively.

creases, the threshold fields decrease— $\overline{H_{\text{th}}^{\text{FC}}} \approx 1.5$ Oe and $\overline{H_{\text{th}}^{\text{ZFC}}} \approx 20$ Oe—and their ratio, which for this sample is $\overline{H_{\text{th}}^{\text{ZFC}}} / \overline{H_{\text{th}}^{\text{FC}}} \approx 13$, increases somewhat. The increase by 1.3 times the value of the ratio $\overline{H_{\text{th}}^{\text{ZFC}}} / \overline{H_{\text{th}}^{\text{FC}}}$ for this case agrees well with the ratio of the average particle radii, which is 1.25, in the experimental samples.

Trapping of magnetic flux in powdered high- T_c superconductors can be observed not only as a change in the hf absorption in zero magnetic field but also as a dependence of the remanent magnetic moment of the sample on the magnetizing field. As shown above, when the trapping of magnetic flux is recorded according to the hf absorption, as shown above, the threshold field can be determined not only for the largest particles but also for particles corresponding to the maximum of the particle-size distribution. On the other hand, when the remanent magnetic moment in weak magnetic fields, corresponding to trapping of individual magnetic vortex filaments, is recorded, the remanent magnetization M_{rem} of the sample increases with H continuously as magnetic flux is trapped successively by increasingly smaller particles. For this reason, the threshold field of only the largest particles can be determined by this method.

Figure 6 shows the field dependence $M_{\text{rem}}(H)$ for a sample with average particle size $S_{\text{av}} \approx 16 \mu\text{m}^2$ after ZFC. Comparing Figs. 4b and 6 shows that the two different methods for determining the field corresponding to trapping of magnetic flux by the largest particle in the powdered high- T_c sample give the same value $H_{\text{th}}^{\text{ZFC}} \approx 10$ Oe.

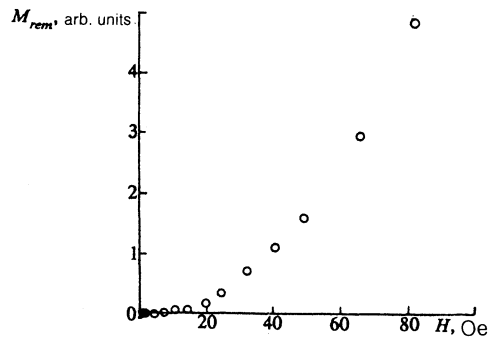


FIG. 6. Remanent magnetization M_{rem} versus the magnetizing field after ZFC for a sample with average particle size of $16 \mu\text{m}^2$.

We note in conclusion that our theoretical analysis of the trapping of magnetic flux in a small high- T_c superconductor was made for $R \ll \lambda$. For the real particle sizes of about $2 \mu\text{m}$ in the samples studied, this condition can be satisfied for $\lambda > 10 \mu\text{m}$. This penetration depth is larger than the values obtained for single crystals.¹¹⁻¹⁴ Nonetheless, as shown above, the theory agrees quite well with our experiments. This can be explained by noting that the actual small particles of the powders of high- T_c superconductors employed in our experiments contain weak links and the real value of λ is an effective penetration depth determined by the network of these weak links. This conclusion is supported by the results of Ref. 15, where it was shown for powders prepared by a similar technology that the approximation $R < \lambda$ likewise gives good agreement between theory and experiment for particles whose average size is less than $5 \mu\text{m}$.

5. CONCLUSIONS

Thus in this work we studied theoretically the trapping of magnetic flux in small high- T_c superconductor samples of different shape. We derived expressions for the threshold magnetic fields corresponding to the formation and trapping of a vortex filament in powdered high- T_c superconductors for the cases of ZFC and FC. These expressions show that the surface barrier plays a significant role in the trapping of magnetic flux in high- T_c superconducting powders initially cooled in zero magnetic field. It was shown that the threshold magnetic fields can be determined from the hf absorption in weak magnetic fields for both the largest particles in the sample and for particles corresponding to the maximum of the particle-size distribution.

We thank M. M. Afanas'ev for assisting in the experiment as well as Professor R. Laikho, director of the Vikhuri Laboratory of the University of Turku (Finland), and E. Lekhderant, our colleague in this laboratory, for making it possible to perform measurements on the SQUID magnetometer.

¹V. Fleisher, E. Lahderanta, R. Laiho, and Yu. P. Stepanov, *Physica C* **170**, 161 (1990).

²M. M. Afanas'ev, E. V. Blinov, L. S. Vlasenko, M. P. Vlasenko, Yu. P. Stepanov, and V. G. Fleisher, *Pis'ma Zh. Eksp. Teor. Fiz.* **51**, 529 (1990) [*JETP Lett.* **51**(10), 600 (1990)].

³A. Dulcic, R. H. Crepeau, and J. H. Freed, *Phys. Rev. B* **39**, 4249 (1989).

⁴K. W. Blazey, A. M. Portic, and F. H. Holzberg, *Physica C* **157**, 16 (1989).

- ⁵Y. Maniva, A. Grupp, F. Hentsch, and M. Merring, *Physica C* **156**, 755 (1988).
- ⁶P. de Gennes, *Superconductivity of Metals and Alloys*, W. A. Benjamin, N.Y., 1966.
- ⁷E. B. Sonin, *Europhys. Lett.* **18**, 69 (1992).
- ⁸M. Konczykowski, L. I. Burlachkov, Y. Yeshurun, and F. Holtzberg, *Phys. Rev. B* **43**, 13707 (1991).
- ⁹L. I. Burlachkov, M. Konczykowski, Y. Yeshurun, and F. Holtzberg, *J. Appl. Phys.* **70**, 5759 (1991).
- ¹⁰M. Foldeaki, M. E. McHenry, and R. C. O'Handley, *Phys. Rev. B* **39**, 2883 (1989).
- ¹¹L. Krusin-Elbaum, A. P. Malozemoff, Y. Yeshurun, D. C. Cronemeyer, and H. Holtzberg, *Phys. Rev. B* **39**, 2936 (1989).
- ¹²L. Fruchter, C. Giovannella, G. Collin, and I. A. Cambell, *Physica C* **156**, 69 (1989).
- ¹³A. Umezava, G. W. Craptree, J. Z. Liu, T. J. Moran, S. K. Malik, L. H. Nunez, W. L. Kwok, and C. H. Sowers, *Phys. Rev. B* **38**, 2843 (1988).
- ¹⁴D. R. Harshman, L. F. Schneemeyer, J. V. Waszczak, G. Aeppli, R. J. Cava, B. Batlogg, L. W. Rupp, E. J. Anasaldo, and D. L. Williams, *Phys. Rev. B* **39**, 851 (1989).
- ¹⁵E. Lahderanta, L. Vlasenko, and R. Laiho, *Physica C* **190**, 497 (1992).

Translated by M. E. Alferieff